Jurnal Geografi Gea

Journal homepage: https://ejournal.upi.edu/index.php/gea

Surface Deformation Analysis Using Differential Interferometry Synthetics Aperture Radar in Rumpin, Cigudeg, Leuwiliang, and Cibungbulang District Period 2018-2022

Rosse Violla Rosendrya[1], Budhi Setiawan[2]

[12]Program Studi Teknik Geologi, Universitas Sriwijaya, Palembang, Indonesia

Correspondence: E-mail: [1]03071281924022@student.unsri.ac.id, [2]budhi.setiawan@unsri.ac.id

ABSTRACT

Ground movement is surface movement resulting from natural events such as landslides, earthquakes, slumping, or surface runoff. Tracking ground movement is a step in mitigating and investigating unexpected natural disasters. Administratively, the research area is in Bogor Regency, namely Rumpin, Cigudeg, Leuwiliang, and Cibungbulang Subdistricts. The area studied by the author is 9 x 9 km². The method uses more than one interferogram to capture surface topographical transformations accurately. The DInSAR method aims to extract the total phase caused by deformation by eliminating or reducing other contributing things. This study identified material movements in the form of decreases or increases. The activity of monitoring material movement is considered essential to be carried out in monitoring potential landslides in the future. SAR imagery can be used as an early warning for disaster mitigation which still requires further action, such as taking data directly to the field in the hope of getting more accuracy.

ARTICLE INFO

Article History:
Submitted/Received 07 Aug 2023
First Revised 13 Sep 2023
Accepted 19 Oct 2023
First Available online 30 Oct 2023
Publication Date 30 Oct 2023

Keyword:
DInSAR,
Sentinel-1,
surface deformation

1. INTRODUCTION

Indonesia that has areas prone to natural disasters. The Regional Disaster Management Agency (BPBD) of Bogor Regency said that out of 40 sub-districts, 22 could be prone to intertwining with medium to large soil movements.

A landslide is surface movement resulting from natural events such as landslides, earthquakes, slumping, or surface flows. (Calò, et al., 2014) (Budetta, 2020). In addition, this can be caused by natural events, such as earthquakes and volcanic eruptions, or human activities, such as the detonation of nuclear weapons. (Niraj, 2022) (Merlín, 2021). Soil movement, grass wasting, is a change in the location of the soil, regolith and rocks caused by the force of gravity with the type of crawl, flow, lying down or falling (Noor, 2014). In several studies, it has been proven that population growth influences surface deformation. (Vélez, 2021) (Samsonov, 2020). Research shows that population growth in recent decades is due to increased demand for food and the development of economic activity. (Ningsih, 2023). This has resulted in more people choosing to live in areas prone to landslides and often compromising natural ecosystems (Arthur Depicker, 2021). The classification of ground movement can be divided based on the main mechanisms involved (creep, flow, slide, heave, fall, and subsidence) and the moisture content of the moving body (very low, low, medium, high, very high, and very high). (Hugget, 2017).

Deformation is a change of form caused by a reaction to the force applied—the styles it defines already and surface forces (Stein, 2003). The method uses more than one interferogram to capture topographic surface transformations accurately. The purpose of using this DInSAR method is to perform total phase extraction caused by deformation by eliminating or reducing other contributing things. (Boni, 2018). This method can be used if at least three radar images or changes in topographic surface nodules can be used as a reference. Interferograms can produce explanations of phases produced by predictions of 2 SARs at different times. The information we get from the interferogram includes topography, orbital displacement, surface deformation, and atmospheric effects (Castañeda, 2011).

The effort to track land movement is a step in mitigating and investigating unexpected natural disasters. (Dini, 2019). Based on this case, this research seeks to share solutions with the DInSAR procedure approach in tracking surface deformation in the 2018–2022 period so that it helps analyse the characteristics of intertwined surface deformations. The DInSAR method can determine the change in the earth's surface by using different phases of electromagnetic waves recorded at two other observation times. (Acosta, et al., 2021). Tracking these deformations provides the geometric state of the deformed object information from the load response (Shan-Long, 1991).

The research area conducted was 9 x 9 km². Based on the stratigraphic sequence of the study area from old to young formations consisting of Bojongmanik Formation (Tmb) with Middle Miocene age, Tuff and Breccia Formation (Tmtb) with Late Miocene age, and Volcanic Breccia (Qvb) with Pleistocene age (Effendi et al, 1998). (**Figure 1**).

DOI: https://doi.org/10.17509/gea.v23i2.61152
p- ISSN 1412-0313 e- ISSN 2549-7529

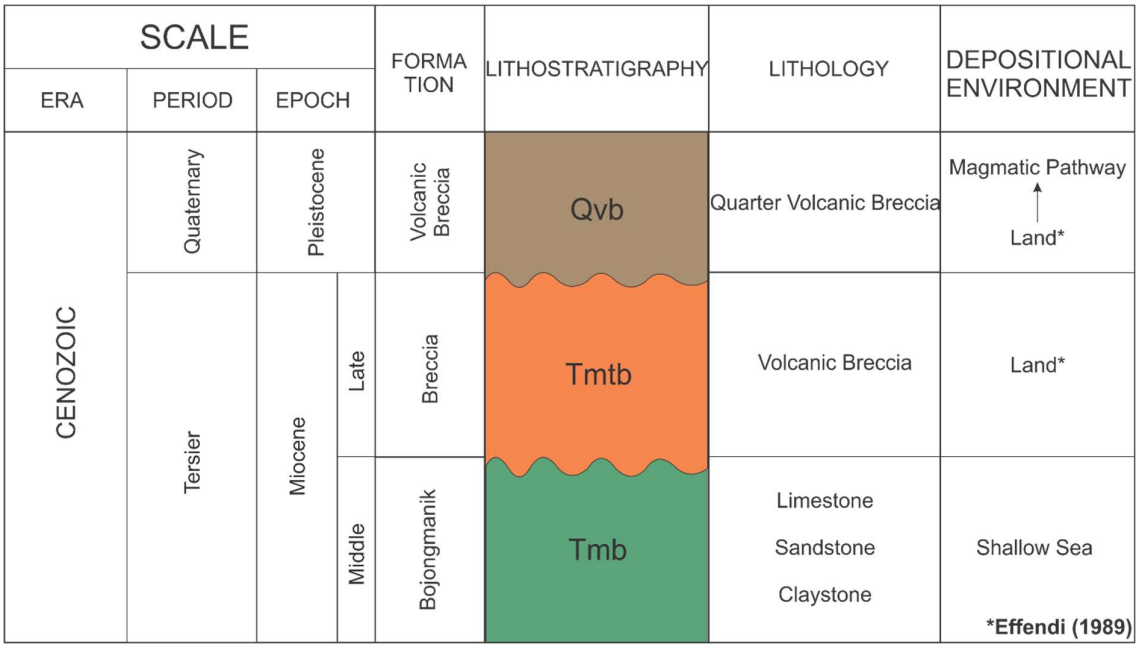

Figure 1. Stratigraphy of Research Area

2. METHODS

The DInSAR method is a side-looking radar imaging that utilises phase, wavelength, and amplitude data (Firdaus, 2016).

This study uses two-path interferometry with the help of the second Shuttle Topographic Radar Mission (SRTM) 3 DEM for the study area. Data sets are required to produce real interferograms at each time interval. Differential interferometric processing aims to separate topographic terms and displacement within an interferogram. (Raspini, 2022). Topographic phases must be omitted to identify the components of displacement. (Sarychikhina, 2021). Therefore, two interferograms are formed. So there are six format interferograms to estimate the displacement during the time interval between the dates of these images. Each aspect is presented to address how to collect and process data. This stage is also expected to produce a research design in the form of a flow chart that can be seen in (**Figure 2**).

The method used in this study is a two-pass DInSAR (Hanssen, 2001), where the equation of at least two phases of the SAR image in the interferogram can be written as follows :

Δ_{φ} = $\varphi_{topo} + \varphi_{defo} + \varphi_{atm} + \varphi_{orb}$ (1)

φ = Different phases

φ_{topo} = Topographic phase

φ_{defo} = Deformation phase

φ_{atm} = Atmospheric phase

φ_{orb} = Orbit phase

DOI: https://doi.org/10.17509/gea.v23i2.61152
p- ISSN 1412-0313 e- ISSN 2549-7529

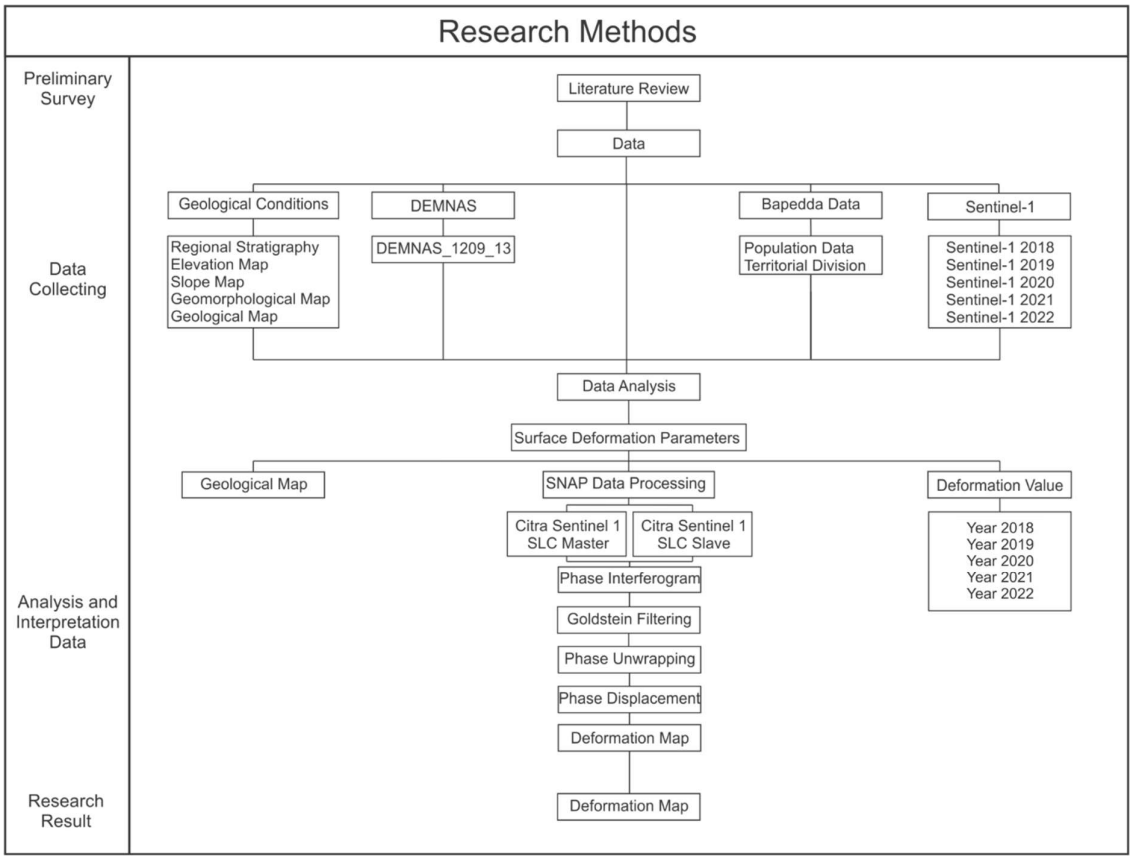

Figure 2. Research Methods

In processing data, researchers use applications that support analysis, including:

Sentinel Application Platform (SNAP)

SNAP is one of the applications used in processing satellite image data, such as Sentinel 1, Sentinel 2, and Sentinel 3 toolbox. This application is used in various other satellite image data processing. This study used SNAP to process sentinel data into interferograms and deformation maps.

Google Earth

Google Earth is an application that can be used in mapping by producing geospatial information that utilises satellite imagery. (Aldiansyah, 2021). In this study, Google Earth was used in processing Sentinel data results to identify areas that have experienced deformation and get the deformation value.

Global Mapper

Global Mapper is software that can be used in satellite image processing. The application can perform topographic analysis, displaying a 3D view of an area. In global research, mappers are used to cut DEM research areas.

Arcgis

ArcGIS is a GIS data processing software that operates in geographic information systems, map creation and analysis, and cartographic creation of maps assisted by supporting features. This research used ArcGIS to make deformation maps for 2018 – 2022 and map cartography.

DOI: https://doi.org/10.17509/gea.v23i2.61152
p- ISSN 1412-0313 e- ISSN 2549-7529

3. RESULTS AND DISCUSSION

The analysis results on the map using DEM (Digital Elevation Model) data show that the study area has an elevation ranging from 50 – 550 meters above sea level. The elevation includes low hills (50-200 meters), hills (200-500 meters) and high hills (500-1000 meters) (Widyaatmanti, 2016). The data is then processed into a three-dimensional form with an elevation index of 50 meters to describe the study area's morphological state and morphological class shape (**Figure 3. A**).

Slope analysis is one of the benchmarks for determining landforms on geomorphological maps of the study area. It was found that the study area was decorated by gentle to rather steep slopes (2%-55%) (**Figure 3. B**).

Based on the results of the analysis by looking at geomorphic aspects and geomorphic processes, it is interpreted that the study area consists of four developing landform units, including the Irrelugar Meander Channel (CIM), Low Slope Gentle Hills (PRL), Pulsed Steep Hills (PCD), and Steep Slope High Hills (PTC) (Widyaatmanti, 2016) (Hugget, 2017). Geomorphological maps of the study area can be viewed in (**Figure 3. C**).

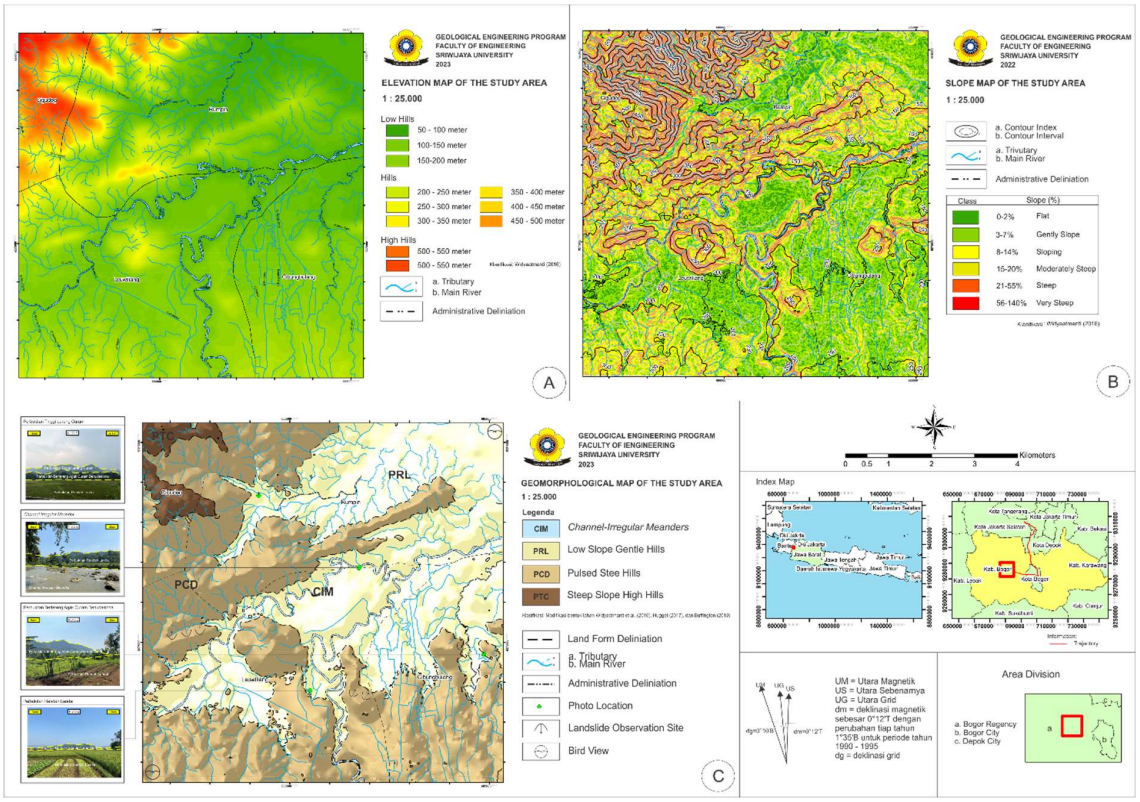

Figure 3. (a) Elevation Map, (b) Slope Map, (c) Geomorphological Map

In the research area, it can be seen that it is controlled by passive morpho-structure, which is a process of changing the earth's surface, which is influenced by the lithology of the study area so that the level of rock resistance determines the degradation process. A process that works passively without movement due to weathering, geological structure, and lithology. In the research area, degradational processes are developed, influenced by rocks' resistance levels. This passive morphostructure process continues until now, supported by avalanches and drags from loose material at several observation points (**Figure 4**). The types of avalanches that occurred in the study area were classified based on (Hugget, 2017).

DOI: https://doi.org/10.17509/gea.v23i2.61152
p- ISSN 1412-0313 e- ISSN 2549-7529

Figure 4. Landslide Evidence in the Research Area

The author uses commands on the Sentinel Application Platform application to process data. The command is created in the graph builder available by inputting data in (**Table 1).**

The results of the unwrapping phase show that the deformation pattern shows a clear and measurable pattern with metric units. Such altered patterns may indicate changes in the shape of the surface of the study area. On the surface of the study area, only part of the area experienced displacement in (**Figure 5**). The number of invaluable pixels is large enough on the surface to make it difficult to read the deformation value caused by the filtering and unwrapping stages. Data coherence values reduce errors when data is hindered by high vegetation density, noise, or scattering errors. The coherence value used is 0.2, so if there is less than 0.2 data, it can reduce the expected error value.

The results of the sorted interferogram show that noise seems to decrease in parts that initially still have medium coherence values. The sorting used in SNAP software is Goldstein Phase Filtering.

Table 1. Sentinel Data in Research Areas

ID Scene	Sentinel 1A	Acquisition	Polarization
S1A_IW_SLC__1SDV_20180112T111433_20180112T111503_020120_0224F1_65B5	Master	12 January 2018	VV + VH
S1A_IW_SLC__1SDV_20181226T111440_20181226T111510_025195_02C8C6_8CD3	Slave	26 December 2018	VV + VH
S1A_IW_SLC__1SDV_20190107T111440_20190107T111510_025370_02CF15_572D	Master	7 January 2019	VV + VH

DOI: https://doi.org/10.17509/gea.v23i2.61152
p- ISSN 1412-0313 e- ISSN 2549-7529

S1A_IW_SLC__1SDV_20191221T111447_20191221T111517_030445_037C21_244F	Slave	21 December 2019	VV + VH
S1A_IW_SLC__1SDV_20200102T111446_20200102T111516_030620_038227_82FB	Master	2 January 2020	VV + VH
S1A_IW_SLC__1SDV_20201227T111453_20201227T111523_035870_04334D_81F8	Slave	27 December 2020	VV + VH
S1A_IW_SLC__1SDV_20210108T111452_20210108T111522_036045_043961_653D	Master	8 January 2021	VV + VH
S1A_IW_SLC__1SDV_20211222T111459_20211222T111528_041120_04E2C3_F472	Slave	22 December 2021	VV + VH
S1A_IW_SLC__1SDV_20220103T111458_20220103T111528_041295_04E8A3_AA15	Master	3 January 2022	VV + VH
S1A_IW_SLC__1SDV_20221205T111506_20221205T111535_046195_0587FF_EF33	Slave	5 December 2022	VV + VH

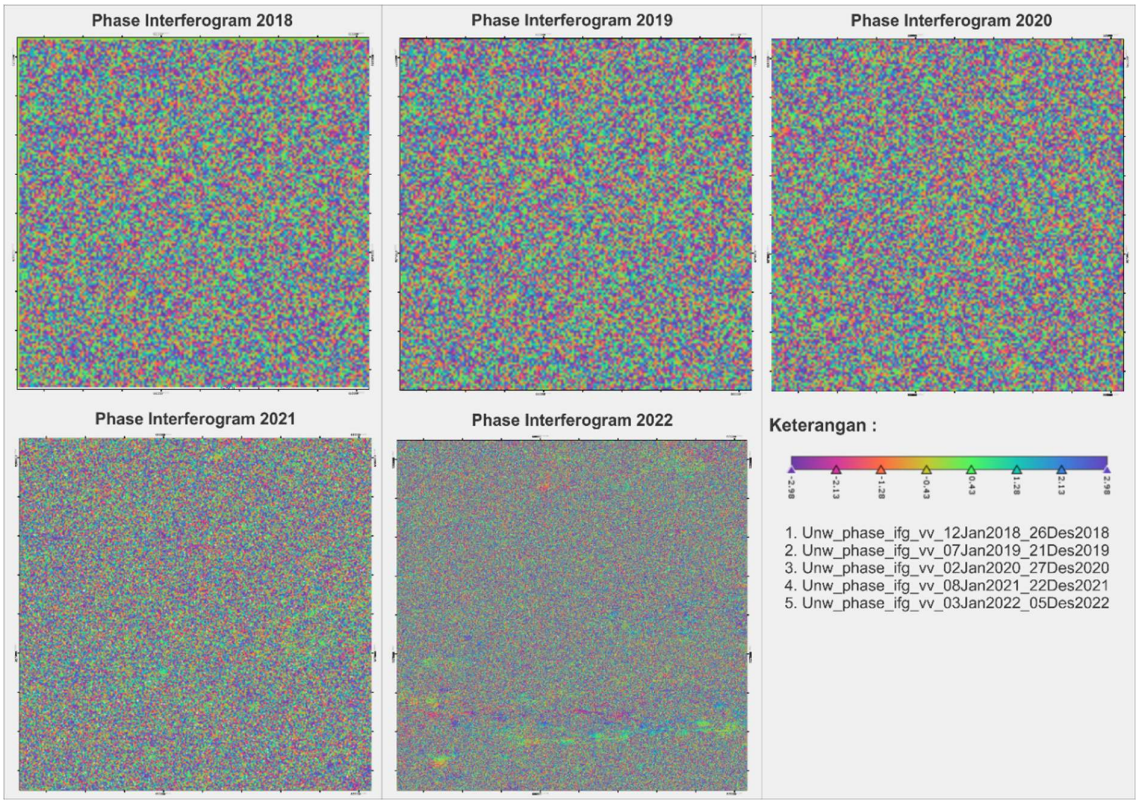

Figure 5. Phase Interferogram

DOI: https://doi.org/10.17509/gea.v23i2.61152
p- ISSN 1412-0313 e- ISSN 2549-7529

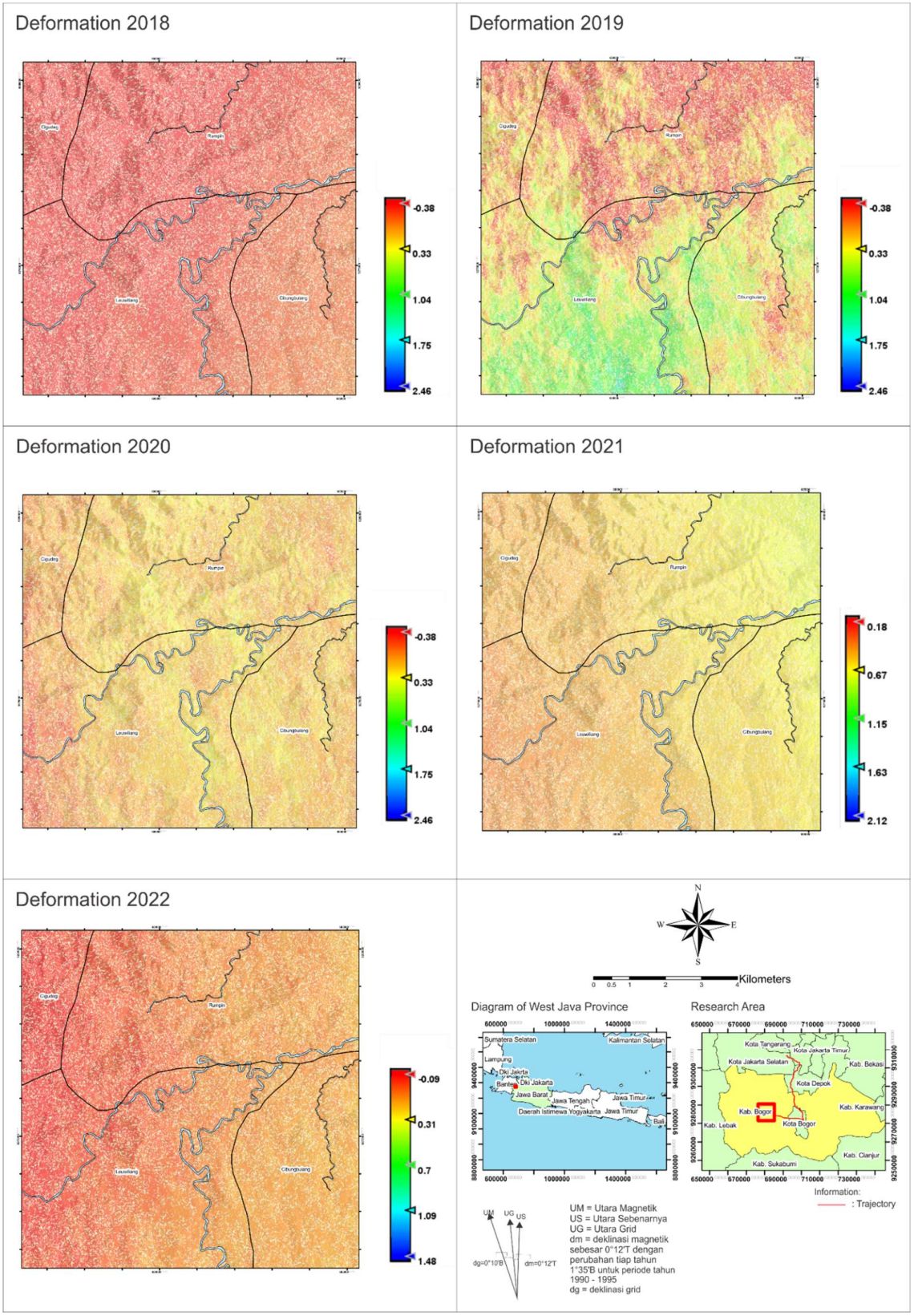

Figure 6. Deformation Map of the Research Area

The results of data analysis that has been carried out using the DInSAR method show that the deformation in the research area has various values from year to year in (**Figure 6**).

DOI: https://doi.org/10.17509/gea.v23i2.61152
p- ISSN 1412-0313 e- ISSN 2549-7529

Deformation that occurs in the study area is divided into two types, namely land level rise (uplift) and land subsidence (subsidence). The land level rise value obtained in the study area was 0.2 cm to 0.67 cm. At the same time, the deformation value that shows land subsidence is at the importance of -0.03 cm to -0.38 cm.

As concluded through (**Table 2**), Rumpin District has a minimum deformation value of 0.67 and a maximum of -0.38, Cigudeg District has a minimum deformation value of 0.42 and a maximum of -0.38, Leuwiliang District has a minimum deformation value of 0.36 and an as maximum As of -0.38. In contrast, Cibungbulang District has a minimum deformation value of 0.67 and a maximum of -0.38.

Changes in surface deformation values can also be caused by increased population each year. (Anjasmara, 2017). Over time, the increasing population will encourage infrastructure development to support population activities in an area so that the land that supports the building can experience subsidence. The population growth of the study area can be seen in (**Diagram 1**).

Table 2. The value of deformation in the research area

District	Deformation/year										Deformation/year
	2018		2019		2020		2021		2022		
	Max	Min	Max	Min	Max	Min	Max	Min	Max	Min	
Rumpin	-0.38	-0.09	-0.258	-0.134	0.07	0.25	0.42	0.67	-0.09	0.2	0.329
Cigudeg	-0.38	-0.3	-0.258	-0.134	0.07	0.16	0.42	0.42	-0.09	-0.06	-0.076
Leuwiliang	-0.38	-0.04	-0.258	-0.134	0.07	0.25	0.36	0.35	-0.09	0.2	0.164
Cibungbulang	-0.38	-0.03	0-.0258	-0.134	0.07	0.25	0.58	0.67	0.2	-0.03	0.598

Diagram 1. Population in 2018-2022 in the Study Area

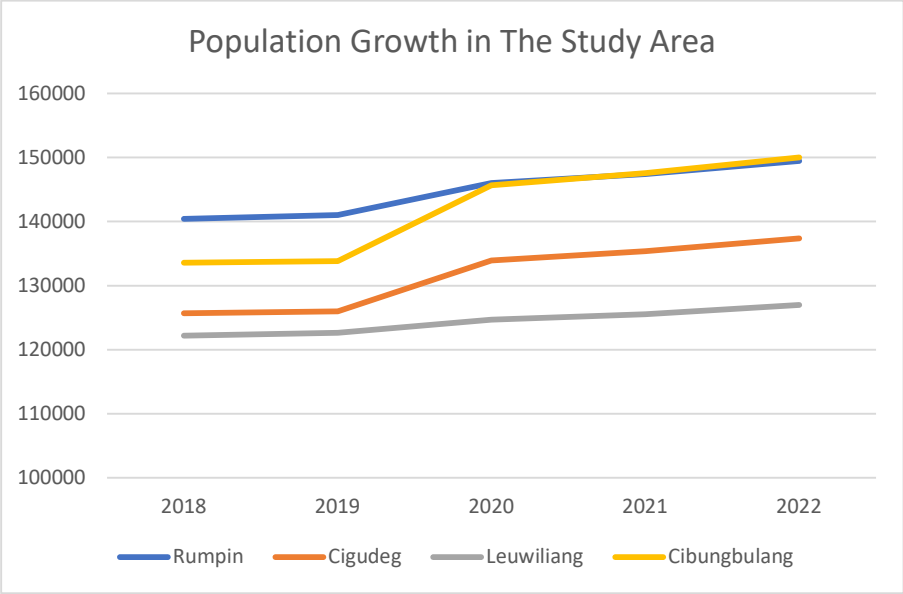

DOI: https://doi.org/10.17509/gea.v23i2.61152
p- ISSN 1412-0313 e- ISSN 2549-7529

4. CONCLUSION

Based on the results of literature studies, data processing, and analysis, it can be concluded that the deformation occurs has diverse values in each region. The Rumpin District area has an average deformation value/year of 0.329 cm, Cigudeg District has an average deformation value/year of -0.076 cm, Leuwiliang District has an average value of deformation/year 0.164 cm, and Cibungbulang District has an average value of deformation/year 0.598 cm.

Factors such as increasing population, development, and sand mining at the research site affect the deformation in the study area. This research can identify material movements in the form of decreases and increases. Material movement monitoring activities are considered essential to be carried out in monitoring possible landslides in the future. SAR imagery can be used as an early warning of disaster mitigation that requires further actions, such as taking data directly to the field for more accurate accuracy.

5. RECOMMENDATIONS

It is recommended to present GPS data accompanied by validation tests to determine the accuracy of the deformation value of the DinSAR method. The pattern of deformation shown in this study still needs to be clarified. This is due to distortions such as temporal decorrelation and geometry that have yet to disappear entirely. Besides, the influence of topography influenced by DEM data has also remained simple.

6. REFERENCES

Acosta, G., Rodriguez, A., Euillades, P., Euillades, L., Ruiz, F., Rosell, P., & Garcia, H. (2021). Detection of Active Landslides by DInSAR in Andean Precordillera of San Juan, Argentina. *Jurnal of South American Earth Sciences, 108*, 103205.

Aldiansyah, S. M. (2021). Monitoring of vegetation cover changes with geomorphological forms using Google Earth engine in Kendari City. *Jurnal Geografi Gea, 21(2)*, 159-170.

Anjasmara, I. M. (2017). Analysing surface deformation in Surabaya from Sentinel-1A data using DInSAR method. *In AIP Conference Proceedings (Vol. 1857, No. 1)*, AIP Publishing.

Arthur Depicker, L. J. (2021). Historical Dynamics of Landslide Risk from Population and Forest-cover Changes in the Kivu Rift. *Nature Sustainability 4*, 965-974.

Boni, R. B. (2018). Landslide state of activity maps by combining multi-temporal A-DInSAR (LAMBDA). *Remote sensing of environment, 217*, 172-190.

Budetta, P. N. (2020). DinSAR monitoring of the landslide activity affecting a stretch of motorway in the Campania region of Southern Italy. *Transportation research procedia, 45*, 285-292.

Calò, F., Ardizzone, F., Castaldo, R., Lollino, P., Tizzani, P., Guzzetti, F., Manunta, M. (2014). Enhanced landslide investigations through advanced DInSAR techniques: The Ivancich case study, Assisi, Italy. *Remote Sensing of Environment, 142*, 69-82.

Castañeda, P. S. (2011). Dedicated SAR interferometric analysis to detect subtle deformation in evaporite areas around Zaragoza, NE Spain. *International Journal of Remote Sensing, 32(7)*, 1861–1884.

Dini, B. M. (2019). nvestigation of slope instabilities in NW Bhutan as derived from systematic DInSAR analyses. *Engineering Geology, 259*, 10511.

Effendi et al. (1998). *Peta Geologi Lembar Bogor, Jawa, skala 1:100.000.* Bandung: Pusat Penelitian dan Pengembangan Geologi.

Firdaus, M. P. (2016). Analisis Pengaruh Deformasi Muka Tanah terhadap Pembangunan di Daerah Pesisir dengan Teknik Differential Interferometric Synthetic Aperture Radar

DOI: https://doi.org/10.17509/gea.v23i2.61152
p- ISSN 1412-0313 e- ISSN 2549-7529

(DInSAR) (Studi Kasus: Pesisir Bangkalan, Madura).

Hanssen. (2001). Radar Interferometry: Data Interpretation and Error Analysis. *Remote Sensing and Digital Image Processing*, 9-60.

Hugget, R. J. (2017). *Fundamental of Geomorphology (4rd edition).* USA and Canada: Routage.

Merlín, A. B. (2021). DInSAR and statistical modeling to assess landslides: The case study of Sierras Chicas (central Argentina). *Journal of South American Earth Sciences, 108*, 103179.

Ningsih, R. L. (2023). Multi-Hazard Susceptibility Analysis of Bantul Regency. *Jurnal Geografi Gea, 23(1)*, 8-18.

Niraj, K. C. (2022). Kotrupi landslide deformation study in non-urban area using DInSAR and MTInSAR techniques on Sentinel-1 SAR data. *Advances in Space Research*, 70(12), 3878-3891.

Noor, D. (2014). *Pengantar Geologi.* Yogyakarta: Deepublish.

Raspini, F. C. (2022). Review of satellite radar interferometry for subsidence analysis. *Earth-Science Reviews*, 104239.

Samsonov, S. D. (2020). Satellite interferometry for mapping surface deformation time series in one, two and three dimensions: A new method illustrated on a slow-moving landslide. *Engineering Geology, 266*, 105471.

Sarychikhina, O. P. (2021). Application of satellite SAR interferometry for the detection and monitoring of landslides along the Tijuana-Ensenada Scenic Highway, Baja California, Mexico. *Journal of South American Earth Sciences, 107*, 103030.

Shan-Long, K. (1991). *Optimization and Designof Deformation Monitoring Schemes.* Canada: Geodesy and Geomatics Engineering.

Stein, W. (2003). An Introduction to Seismology, Earthquakes, and Earth Structure. *Geological Magazine*, 733-734.

Vélez, M. L. (2021). Ground deformation at the Cerro Blanco caldera: A case of subsidence at the Central Andes BackArc. *Journal of South American Earth Sciences, 106*, 102941.

Widyaatmanti, W. I. (2016). *Identification of topographic elements composition based on landform boundaries from radar interferometry segmentation (preliminary study on digital landform mapping).* IOP Conference Series: Earth and Environmental Science, 37(1).

DOI: https://doi.org/10.17509/gea.v23i2.61152
p- ISSN 1412-0313 e- ISSN 2549-7529